

Serial Analysis of Gene Expression in Circulating $\gamma\delta$ T Cell Subsets Defines Distinct Immunoregulatory Phenotypes and Unexpected Gene Expression Profiles

This information is current as of August 9, 2022.

Nicole Meissner, Jay Radke, Jodi F. Hedges, Michael White, Michael Behnke, Shannon Bertolino, Mitchell Abrahamsen and Mark A. Jutila

J Immunol 2003; 170:356-364; ;
doi: 10.4049/jimmunol.170.1.356
<http://www.jimmunol.org/content/170/1/356>

References This article **cites 50 articles**, 19 of which you can access for free at:
<http://www.jimmunol.org/content/170/1/356.full#ref-list-1>

Why *The JI*? [Submit online.](#)

- **Rapid Reviews! 30 days*** from submission to initial decision
- **No Triage!** Every submission reviewed by practicing scientists
- **Fast Publication!** 4 weeks from acceptance to publication

**average*

Subscription Information about subscribing to *The Journal of Immunology* is online at:
<http://jimmunol.org/subscription>

Permissions Submit copyright permission requests at:
<http://www.aai.org/About/Publications/JI/copyright.html>

Email Alerts Receive free email-alerts when new articles cite this article. Sign up at:
<http://jimmunol.org/alerts>

Serial Analysis of Gene Expression in Circulating $\gamma\delta$ T Cell Subsets Defines Distinct Immunoregulatory Phenotypes and Unexpected Gene Expression Profiles

Nicole Meissner,* Jay Radke,* Jodi F. Hedges,* Michael White,* Michael Behnke,* Shannon Bertolino,[†] Mitchell Abrahamsen,[†] and Mark A. Jutila*

Gene expression profiles were compared in circulating bovine GD3.5⁺ (CD8⁻) and GD3.5⁻ (predominantly CD8⁺) $\gamma\delta$ T cells using serial analysis of gene expression (SAGE). Approximately 20,000 SAGE tags were generated from each library. A comparison of the two libraries demonstrated 297 and 173 tags representing genes with 5-fold differential expression in GD3.5⁺ and GD3.5⁻ $\gamma\delta$ T cells, respectively. Consistent with their localization into sites of inflammation, GD3.5⁺ $\gamma\delta$ T cells appeared transcriptionally and translationally more active than GD3.5⁻ $\gamma\delta$ cells. GD3.5⁻ $\gamma\delta$ T cells demonstrated higher expression of the cell proliferation inhibitor BAP 37, which was associated with their less activated gene expression phenotype. The immune regulatory and apoptosis-inducing molecule, galectin-1, was identified as a highly abundant molecule and was higher in GD3.5⁺ $\gamma\delta$ T cells. Surface molecules attributed to myeloid cells, such as CD14, CD68, and scavenger receptor-1, were identified in both populations. Furthermore, expression of B lymphocyte-induced maturation protein, a master regulator of B cell and myeloid cell differentiation, was identified by SAGE analysis and was confirmed at the RNA level to be selectively expressed in $\gamma\delta$ T cells vs $\alpha\beta$ T cells. These results provide new insights into the inherent differences between circulating $\gamma\delta$ T cell subsets. *The Journal of Immunology*, 2003, 170: 356–364.

The $\gamma\delta$ T cells were first identified 16 years ago (1, 2), and since then considerable effort has been devoted to understanding their function and importance in human and animal health. Although low in number in the peripheral blood, these cells are maintained in every animal with a complex immune system emphasizing their importance as a functional entity. A consensus concerning their role, however, has not been established. An interesting aspect of these cells that has come from studies in mice, humans, and cattle is that discrete subsets of these cells, defined by their TCR usage, as well as certain differentiation markers accumulate in different tissues (3–10). Recent findings demonstrate that tissue-specific subsets have different functions, with some being proinflammatory and others being anti-inflammatory (11, 12). Also, subsets respond to infectious challenge differently. For example, removal of the V γ 1 subset improves the ability of mice to clear *Listeria monocytogenes* infection, whereas depleting all $\gamma\delta$ T cells has the opposite effect (13). Conversely, in coxsackie virus infection, depletion of the V γ 1 subset results in an exacerbation of the infection-induced myocarditis. On the other hand, removal of V γ 4 cells reduces the inflammatory damage caused by infection (14). It is likely that some of the inconsistency in the literature concerning $\gamma\delta$ T cells is due to the analysis of mixed

populations of cells that contain subsets with opposing activities. Therefore, to fully understand $\gamma\delta$ T cell populations as a whole, experiments must include analyses of individual subsets.

Some differences in $\gamma\delta$ T cell subsets isolated from tissues are caused by influences of local growth and activating factors. However, many differences are due to inherent differences in the subsets themselves. Various tissue-specific $\gamma\delta$ T cell subsets can be found in the circulation, thus some of the confounding effects of tissue microenvironments on T cells can be avoided by analyzing these cells. However, the analysis of circulating $\gamma\delta$ T cells can be difficult due to their low numbers in the peripheral blood of most mammals (usually 1–10%). In contrast, newborn ruminants, such as 1- to 6-mo-old calves, have 30–70% circulating $\gamma\delta$ T cells (15); making them a useful animal model for these types of studies. As in other mammals, the majority of bovine $\gamma\delta$ T cells are negative for CD4 and CD8. However, one $\gamma\delta$ T cell subset is of particular interest because of its coexpression of CD8 and CD2, both functionally important accessory molecules, and lack of GD3.5 Ag. Bovine CD8⁺, GD3.5⁻ $\gamma\delta$ T cells are found in low numbers in blood and in high numbers in mucosal sites and the red pulp of the spleen (8). Conversely, CD8⁻, GD3.5⁺ $\gamma\delta$ T cells are found predominantly in the white pulp of the spleen, peripheral lymphoid tissues, sites of inflammation, and the blood (16). The unique distribution of these subsets suggests that their functions are different, although a comprehensive comparison has not been performed.

High throughput sequencing of expressed sequence tags (ESTs) and/or hybridization of gene arrays allows for a comprehensive analysis of global gene expression in cells and can provide insights into novel cellular functions. Serial analysis of gene expression (SAGE)³ or Affymetrix high density oligonucleotide arrays have been applied to the study of different T cell subsets, including $\gamma\delta$

*Veterinary Molecular Biology, Montana State University, Bozeman, MT 59717; and [†]Department of Veterinary Pathobiology, University of Minnesota, St. Paul, MN 55108

Received for publication June 6, 2002. Accepted for publication November 4, 2002.

The costs of publication of this article were defrayed in part by the payment of page charges. This article must therefore be hereby marked *advertisement* in accordance with 18 U.S.C. Section 1734 solely to indicate this fact.

¹ This work was supported by the U.S. Department of Agriculture Initiative Future Agriculture and Food Safety program (2000-04446) and the Murdock Charitable Trust. It is manuscript 2002-36 from the Montana Agricultural Experiment Station.

² Address correspondence and reprint requests to Dr. Mark A. Jutila, Veterinary Molecular Biology, Montana State University, Bozeman, MT 59717. E-mail address: uvsmj@montana.edu

³ Abbreviations used in this paper: SAGE, serial analysis of gene expression; BLIMP-1, B lymphocyte-induced maturation protein-1; EST, expressed sequence tag; HS, horse serum; IEL, intraepithelial lymphocyte.

T cells. Fahrner and colleagues (17) compared gene expression patterns of tissue-specific, resting $\gamma\delta$ intraepithelial lymphocytes (IELs) vs cells following *Yersinia* infection, and identified unexpected regulated genes important in lipid metabolism, cholesterol homeostasis, and physiology. Recently, using SAGE (18), Shires et al. (19) characterized an activated, yet resting phenotype of murine $\gamma\delta$ IELs, due to the high expression of molecules, such as granzymes and Fas ligand, and the low expression of conventional cytokines and their receptors. To date, there have been no reported functional genomic analyses of circulating $\gamma\delta$ T cells. In this report we describe a SAGE analysis of circulating GD3.5⁺ and GD3.5⁻ bovine $\gamma\delta$ T cells, which are also distinguished by CD2/CD8 expression, to analyze their functional potential before being recruited to a specific tissue site. Results showed a surprising number of differentially expressed genes that provide new insights into the functional differences of these $\gamma\delta$ T cell subsets and the relationship of these cells to myeloid cells.

Materials and Methods

Animals and cells

Holstein calves were purchased from local producers and housed at the Montana State University large animal facilities at the Veterinary Molecular Biology Laboratory. Cattle used in this study were bull calves from 1–4 mo of age. Peripheral blood was collected into sodium heparin anticoagulant tubes by venipuncture, and PBMC were purified by Histopaque 1077 (Sigma-Aldrich, St. Louis, MO) gradient centrifugation.

Abs and FACS analysis

The following mouse mAbs, whose staining patterns on bovine $\gamma\delta$ T cells have been previously characterized (8, 16, 20, 21), were used in these studies. GD3.8 recognizes $\gamma\delta$ TCR (8). GD3.5 recognizes nearly all CD8⁻ $\gamma\delta$ T cells, but not CD8⁺ $\gamma\delta$ T cells (8, 16, 20). CC58 recognizes bovine CD8, and CC42 recognizes bovine CD2 (21). MHM23 recognizes bovine CD18 (DAKO, Glostrup, Denmark). H58A (anti-bovine MHC class I), CACT116A (anti-bovine IL-2R), and BAT31A (anti-bovine CD44) were obtained from VMRD (Pullman, WA). Some mAbs were directly conjugated to FITC, PE, or biotin for multicolor flow cytometric analysis. Second-stage reagents included PE-conjugated anti-mouse IgG (Jackson ImmunoResearch Laboratories, West Grove, PA) and avidin-conjugated CyChrome (BD Pharmingen, San Diego, CA).

Multicolor flow cytometric analysis was performed as follows. One hundred microliters of hybridoma supernatant fluid or purified mAb at a final concentration of 20–50 $\mu\text{g/ml}$ was incubated with cells for 30 min on ice and then washed from the cells with PBS containing 5% horse serum (Sigma-Aldrich; PBS-HS). PE-labeled second-stage, diluted 1/250 in PBS-HS was then added and incubated for 30 min on ice. The samples were washed with PBS-HS, incubated in 10% mouse serum in PBS for 15 min, and washed again. As an example of a three-color stain, biotin-labeled GD3.8 (anti-pan $\gamma\delta$ T cell mAb) and FITC-conjugated CC58 (anti-CD8) were added, and the cells were incubated on ice for 30 min. Cells were washed in PBS-HS and incubated with avidin-CyChrome diluted 1/2000 in PBS-HS. After 30 min on ice, the cells were washed in PBS-HS and analyzed using a FACSCalibur (BD Biosciences, Mountain View, CA). The 488-nm laser and FL1 (FITC), FL2 (PE), and FL3 (CyChrome) detectors were used. The FACSCalibur was calibrated using Calibright beads (BD Biosciences). Compensation was set manually using single-color stains of the various fluorochromes. Data from up to 50,000 cells were acquired. Negative controls included 1) single-color stains, 2) irrelevant isotype-matched Ab stains, and 3) second-stage reagent controls. For statistical analysis, markers were placed just above the upper limit of background staining of control Abs.

Cell sorting

For high speed cell sorting of CD8⁺ and CD8⁻ $\gamma\delta$ T cells, two different staining protocols were used based on our previous studies (8, 16). In one, GD3.8 (anti- $\gamma\delta$ T cell) and CC58 (anti-CD8) were used in a two-color stain to detect the two populations. In the other, GD3.8 was combined with GD3.5, which stains CD8⁻ $\gamma\delta$ T cells (8, 16, 20). CD8⁺ $\gamma\delta$ T cells express lower levels of TCR, and this characteristic was also used in restricting the sort gates to ensure the purest population possible (16) (see *Results*). To obtain sorted $\gamma\delta$ T cells vs enriched $\alpha\beta$ T cells, PBMC were stained using GD3.8 Ab (total $\gamma\delta$ T cells) vs an FITC-labeled CC42 Ab (CD2⁺ cells)

(20). All GD3.8-positive cells were included in the $\gamma\delta$ T cell sort, whereas the $\alpha\beta$ T cells included only CD2⁺ GD3.8⁻ cells (all bovine $\alpha\beta$ T cells express CD2). High speed cell sorting was performed on a Vantage SE cell sorter equipped with Turbo Sort (BD Biosciences). Sort rates ranged from 10,000–20,000 cells/s. The purity of each sort was confirmed by analyzing samples on a FACSCalibur, as described above. CD8⁺ $\gamma\delta$ T cells ranged from 1–5% of the starting population in each sort and were the limiting cell population. Cell yields ranged from 1×10^6 to 2×10^7 cells/sort from ~100 ml of blood.

RNA isolation and RT-PCR analysis

Sorted cells were seeded in 24- or 6-well culture plates (Costar, Cambridge, MA) at a concentration of $1 \times 10^6/\text{ml}$ and were cultured overnight at 37°C in 5% CO₂ in RPMI containing 10% FCS. The following day, cells were stimulated for 3.5 h with 20 ng/ml of PMA (Sigma-Aldrich) and 0.5 $\mu\text{g/ml}$ of ionomycin (Sigma-Aldrich). Cells were then washed with HBSS and pelleted by centrifugation, and total RNA was isolated using the TRIzol reagent (Life Technologies, Gaithersburg, MD), according to the manufacturer's protocol. The RNA from at least three sorts of blood from different calves (at least 1×10^6 sorted cells for each subset from each animal) was combined for further analysis. The pooled RNA was treated with DNase, extracted again with phenol/chloroform, and used in real-time PCR analysis. RT was performed with Superscript RT, random primers (Invitrogen, San Diego, CA), and 300 ng sample (CD8⁺ or CD8⁻ $\gamma\delta$ T cell) RNA according to the manufacturer's protocol. Relative specific mRNA in the CD8⁺ and CD8⁻ $\gamma\delta$ T cells was quantified by measuring SYBR green incorporation during real-time quantitative PCR using the relative standard curve method. Bovine sequences were analyzed using Primer Express software (PE Applied Biosystems, Foster City, CA) to design optimal real-time PCR primers (Table I). Primers specific for bovine 18S RNA were used as the endogenous control. Standard curves were constructed using serially diluted, similarly extracted, total bovine PBL RNA. One microliter of each RT reaction was used in the 25 μl real-time PCR reactions, which were performed in triplicate. The PCR was set up and cycled, data were collected on the GeneAmp 5700 Sequence Detection System (PE Applied Biosystems), and calculations were performed as described in the manufacturer's protocol and in User Bulletin 2 for the ABI PRISM 7700 Sequence Detection System. Statistical significance of differential expression was determined for each primer set using Student's *t* test. PCR products (ornithine decarboxylase, IL-1 β , selenoprotein T, Bcl-x_L, JunB, B lymphocyte-induced maturation protein-1 (BLIMP-1), and CD14) were confirmed by sequence analysis.

A semiquantitative RT-PCR method with limited amplification of specific cDNA products was also used in some confirmation experiments and was performed as previously described (22, 23). Gene-specific amplification was performed for the listed genes and corresponding primer sets listed in Table I. Primers were based on bovine EST data from the National Center for Biotechnology Information data bank as well as based on published sequences (24, 25).

SAGE library construction and analysis

Due to the relatively low numbers of sorted CD8⁺ $\gamma\delta$ T cells that could be obtained, SAGE libraries were constructed by template switching and PCR amplification, as previously described (26). Briefly, a biotinylated oligo(dT) primer (biotin-5'-AAGCAGTGGTAACAACGCAGAGTAC(T)₃₀VN-3', where V = A, C, or G, and N = T, C, G, or A) and Superscript II reverse transcriptase (Invitrogen) were used to make first-strand cDNA from 100 ng of total RNA. Second-strand synthesis and cDNA amplification were completed by PCR using Advantage2 Polymerase Mix (Clontech, Palo Alto CA) and a switching primer (5'-AAGCAGTGGTAACAACGCAGAGTACGCGGG-3') in combination with the original biotinylated oligo(dT). SAGE library construction was completed using 5 μg of the ds-cDNA following standard protocols (19, 27, 28). Large-scale sequencing of concatemeric di-tags was completed at the University of Minnesota sequencing facility (Veterinary Pathobiology, Minneapolis, MN) and the U.S. Department of Agriculture Meat Animal Research Center (Clay Center, NE). Tag frequencies were analyzed using the SAGE software package (version 4.05) (19) and a relational database (ACCESS; Microsoft, Redmond, WA). Genes represented by tag sequences from the analysis were identified by direct comparison with annotated 3'-specific tag sequences extracted from the available *Bos taurus* ESTs. To provide current sequence annotation, bovine ESTs were first BLASTed locally against the nonredundant nucleotide and protein databanks obtained from National Center for Biotechnology Information (<http://www.ncbi.nlm.nih.gov>).

Table I. Primer sets used for PCR analysis

	Forward Primer	Reverse Primer
Semiquantitative PCR		
γ -Actin (420 bp)	ACCAACTGGGACGACATGGA	GAGCTTCTCCTTGATGTCAC
L-Selectin (413 bp)	GGAAATCTGGACAATGCTCTGTGTGATT	GGAAATTCGCAAGAAGCTGTGTAACGGGCTT
Tristetraprolin (402 bp)	GCGACTTCCCATCTTCAATC	GGCTCCAATCACCAGACACT
Galectin 1 (403 bp)	CAATCATGGCTGTGGTCTG	GGCCACACACTTGATCTTGA
CCR4, nocturnin (391 bp)	TTCTGAAACATCCCTGGTT	ATTCCCTGATTGTTTGTGG
Bcl-x _L (397 bp)	ATCAATGGCAACCCATCCT	TGGATCCAAGGCTCTAGGTG
IL-1 β (385 bp)	AAGGCTCTCCACCTCTCTC	CCCTGGGTATGGCTTTCTTT
Selenoprotein T (385 bp)	AGACATCCGCATTGAAGGAG	ATGATCGATGTTGTGGGATT
β -Actin (396 bp)	GGCACCACACCTTCTACAAT	ACGTAGCACAGCTTCTCCTT
Real-time quantitative PCR		
CD14	TGAACATTGCCCAAGCACAC	GCCGAGACTGGGATTGTGTCAG
BLIMP-1	GACATGGAGGACCGGATAT	CCTTCCACACAGAATCCCA
Galectin 1	TCATGGCTTGTGGTCTGGTC	CAGCAAGAAGCTCTTGGCGT
Bcl-x _L	ATCACCCAGGACAGCATA	CCGAAGGAGAAAAGGCCAC
Selenoprotein T	AAAGATGCAGTACGCCACGG	GCTGGCTAATAACCCGCATG
Ornithine decarboxylase	GCGGAGTTTTGTCTGTTT	TCCCTTCCTCTCTGTCG
JunB	TGGACGACCTGCACAAGATG	GCAGAGGCCGGAGAATAGCT
IL-1 β	ATAACCCCGAGGACTGGCAG	AGCACTAATGCAGGGAAGGC

RNase protection assay

Total $\gamma\delta$ T cells and $\alpha\beta$ -enriched lymphocytes were sorted as described above. RNA was isolated from 4-h PMA/ionomycin-stimulated, unsorted PBMC; total $\gamma\delta$ T cells; and $\gamma\delta$ -depleted, $\alpha\beta$ -enriched lymphocytes (CD2⁺, GD3.8⁻). Bovine BLIMP-1 primers were designed based on sequence homology of a bovine EST to human and mouse BLIMP-1 (National Center for Biotechnology Information accession no. NP-031574; gb BE483183.1) (5'BLIMP-1, CCAGTGCTGTGAAGGTTCCA; 3'BLIMP-1, AGCTCCCC TCTGGAATAG; PCR size, 420 bp), and an *RsaI/Sau3a* restriction digest for directional cloning into the *SmaI/Bam*HI-digested pBS vector (Stratagene, La Jolla, CA) was performed, generating a 236-bp fragment. The pBS-BLIMP-1 construct was linearized with *EcoRI* for in vitro transcription of an antisense RNA probe using T3 RNA polymerase (Roche, Indianapolis, IN) in a 20- μ l reaction volume with 1 \times transcription buffer (10 mM DTT, 0.3 mM cold rNTP mix (rATP, rCTP, rGTP), 2.5 μ M cold rUTP, 50 μ Ci of [α -³²P]UTP, and 0.6 μ l of RNasin) at 37°C for 1 h. For DNA digest, 25 μ g of yeast RNA and 5 μ l of RQ1 DNase (Promega, Madison, WI) were added and incubated for 30 min at 37°C. The reaction was stopped with 150 μ l of TES (10 mM Tris (pH 7.5), 5 mM EDTA, and 1% SDS) and unincorporated nucleotides were removed using a 5-ml Sephadex G-50 fine column. As a standard curve, declining concentrations of 4-h PMA/ionomycin-activated bovine PBMC-RNA (10 to 0.1 μ g) were used and compared with 1 μ g of $\gamma\delta$ and $\alpha\beta$ T cell RNA. For hybridization, yeast RNA was added to the standard and sample RNAs for a final amount of 50 μ g of RNA (e.g., 1 μ g of sample RNA plus 49 μ g of yeast RNA). Yeast RNA alone was used as a negative control in the hybridization reactions. Five femtomoles of labeled antisense BLIMP-1 RNA probe was used in the hybridization procedure. Probe and samples were mixed, lyophilized,

and then hybridized in 30 μ l of hybridization buffer (80% deionized formamide, 40 mM PIPES (pH 7.0), 400 mM NaCl, 1 mM EDTA, in 0.1 \times TES) at 55°C for 18–24 h. For RNase digestion, tubes were centrifuged, and 390 μ l of RNase mix (10 μ g/ml of RNase A (Roche) and 0.35 U/ μ l of RNase T1 (Roche)) in 1 \times RNase digestion buffer (10 mM Tris (pH 7.5), 5 mM EDTA, and 300 mM NaCl) was added and incubated for 1 h at 37°C. RNase digestion was terminated by adding 25 μ l of proteinase K mix (1 μ g/ μ l of proteinase K and 0.5 μ g/ μ l of yeast RNA in 10 \times TES buffer) and was incubated for 15 min at 37°C. Samples were phenol/chloroform-extracted, ethanol-precipitated, and separated on a 5% denaturing acrylamide gel. The gel was dried and exposed to x-ray film for 1–3 days.

Results

High speed cell sorting of $\gamma\delta$ T cell subsets and SAGE library construction

Using the different staining procedures outlined in *Materials and Methods*, we found that the best purity of CD8⁺ $\gamma\delta$ T cells was achieved when using GD3.8 and GD3.5 Ab staining. This is because CD8 surface expression on $\gamma\delta$ T cells was too low to achieve a clean sort at rates >10,000 cells/s (purities were <70% when sorting using anti-CD8; data not shown). Using the higher intensity of the GD3.5 stain combined with the stain for TCR provided a sorting effectiveness approaching 100% (Fig. 1A). Phenotypic analysis of the sorted populations showed that the GD3.5⁻, low

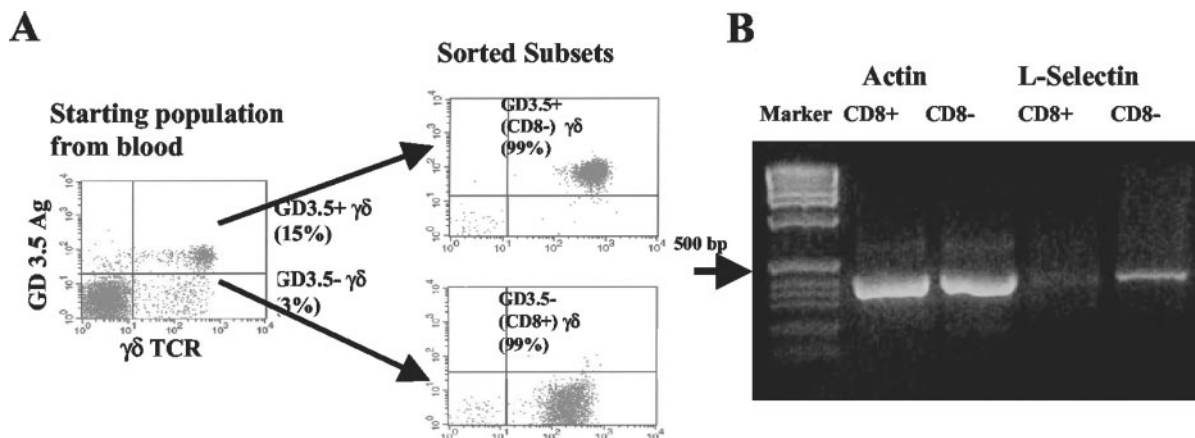


FIGURE 1. Sorting effectiveness and selective expression of L-selectin mRNA in GD3.5⁺ (CD8⁻) vs GD3.5⁻ (CD8⁺) $\gamma\delta$ T cells. *A*, A representative sort using GD3.8-FITC ($\gamma\delta$ TCR/x-axis) and GD3.5 PE (GD3.5 Ag expressed on CD8⁻, but not on CD8⁺, $\gamma\delta$ T cells/y-axis). *B*, A PCR analysis of the amplified cDNA from the sorted cells showing that L-selectin was preferentially expressed in the GD3.5⁺, CD8⁻ $\gamma\delta$ T cell sample.

TCR cells were CD2⁺ and >90% CD8⁺, and the GD3.5⁺ cells lacked CD2 and CD8 (data not shown) (8, 16, 20, 29). Because of our past (16) and current focus on CD8, we refer to these subsets as being either CD8⁺ or CD8⁻ $\gamma\delta$ T cells.

To address changes in gene expression that resulted from the sorting procedure (some cytokine transcript levels were greatly reduced following sorting; data not shown), and to ensure maximum gene expression for SAGE analysis, the sorted cells were cultured overnight and then stimulated for 3.5 h with PMA/ionomycin. We previously showed that this procedure induced transcripts for IFN- γ , lymphotactin, TNF- α , and IL-4 (N. Meissner and M. A. Jutila, unpublished observations). Amplified cDNA was generated, and differential gene expression of L-selectin, which we have previously shown to be selectively expressed on CD8⁻ $\gamma\delta$ T cells (16), was measured by RT-PCR of the same sample as that used for SAGE library construction. As shown in Fig. 1B, a greater amount of L-selectin PCR product was amplified from the CD8⁻ vs the CD8⁺ $\gamma\delta$ T cell library.

A total of 42,910 SAGE tags from both libraries were generated for this initial evaluation. This provided 10,460 and 6,634 tags with unique sequences for the CD8⁺ and CD8⁻ libraries, respectively (Table II). At this level of coverage, many sequences were represented by only one tag. Of all unique tags, 1118 had a frequency of more than five tags. More than 60% of these tags matched at least one bovine EST present in either the TIGR, UNIGENE, or a bovine EST database available at National Center for Biotechnology Information (data not shown). A surprising number of genes were differentially expressed in activated CD8⁺ and CD8⁻ $\gamma\delta$ T cells (Table II). There were 173 and 297 distinct sequences differentially expressed by 5-fold or more in CD8⁺ and CD8⁻ $\gamma\delta$ T cell subsets, respectively. These numbers were reduced to 34 and 77, respectively when considering differences >10-fold. Overall, ~2,000 unique tags from each library matched at least one EST; however, far more tags had no match in the genome databases. Thus, there was no reason at this time to sequence deeper into the libraries, and the current level of coverage was used to compare the two subsets. Complete listings of all tags and corresponding blast results can be found at: <http://vmbmod10.msu.montana.edu/vmb/jutila-lab/SageBovine.htm>.

Before extensive analysis of the SAGE results, confirmation experiments were performed on a select number of genes representing activation/proliferation, cytokine, cell surface, and immunoregulatory molecules identified in the initial annotation of the SAGE tags. Real-time RT-PCR analysis, semiquantitative RT-PCR, and flow cytometry (when bovine-specific Abs were available) were used to confirm gene expression patterns for 16 gene products. Although the extent of regulation varied, real-time quantitative RT-PCR data were consistent with our SAGE analysis for six of eight selected genes analyzed by this approach (Fig. 2). Although the selective expression of selenoprotein T predicted by SAGE was seen in the real-time RT-PCR, the difference was not significant ($p < 0.5$; Fig. 2). All other confirmed differences were significant ($p < 0.05$ or $p < 0.01$).

Table II. Summary of SAGE analysis from sorted CD8⁺ vs CD8⁻ $\gamma\delta$ T cells

	CD8 ⁺	CD8 ⁻
Total tags/library	20,124	22,786
No. of unique tags	10,476	6,634
No. of tags matched to UNIGENE ^a	685	791
No. of tags matched to TIGR ^a	2,187	1,977
No. of tags with ≥ 5 -fold difference between subsets	173	297
No. of tags with ≥ 10 -fold difference between subsets	34	77

^a Numbers include tags that have more than one UNIGENE or TIGR description.

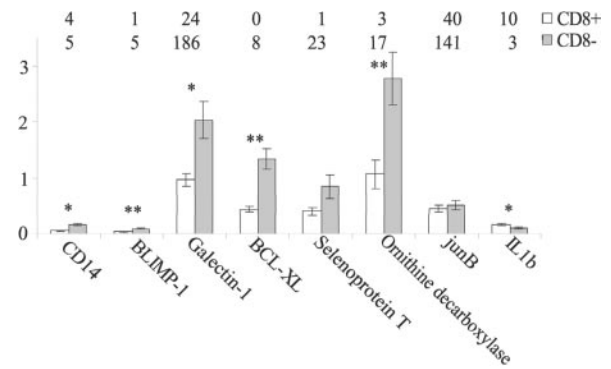


FIGURE 2. Real-time RT-PCR analysis of differentially regulated genes predicted by SAGE. Real-time RT-PCR was performed on select genes as described in *Materials and Methods*. The analysis was performed in triplicate, and the mean \pm SEM are shown. The corresponding SAGE tag frequencies are shown immediately above the RT-PCR data for each gene. Real-time RT-PCR differences are indicated: *, $p < 0.01$; **, $p < 0.05$.

0.01). Semiquantitative RT-PCR results were consistent for nocturnin (CCR4), IL-2R, galectin-1, IL- β , and selenoprotein T, but not Bcl-x_L (data not shown). Table III shows a comparison of SAGE tag frequency to the levels of MHC I, CD44, CD18, IL-2R α -chain, and TCR on $\gamma\delta$ T cells as estimated by FACS analysis, again consistent with the SAGE analysis. Protein expression profiles are shown from unactivated and 24-h PMA/ionomycin-stimulated cells (minimal surface changes were detected at 3.5 h; data not shown). Our staining for CD18, IL-2R, and TCR were consistent with our previous studies (16, 24) (E. Wilson, unpublished observations). MHC I has been previously shown to be homogeneously expressed on bovine lymphocytes (30). These results demonstrate that SAGE is a reliable predictor of gene regulation in this system, particularly for differences in SAGE that are ≥ 5 -fold.

Expression of genes involved in cell activation, transcription, and translation regulation and protein processing in CD8⁻ $\gamma\delta$ T cells vs CD8⁺ $\gamma\delta$ T cells as predicted by SAGE

With few exceptions, the most abundant tags were general housekeeping genes, coding for ribosomal proteins, histones, and transcription and translation initiation factors (Table IV). One striking exception was connexin 43, a gap junction protein. Although both cell subsets were stimulated in the same fashion, out of 100 genes identified by SAGE involved in cellular activation, 37 genes were 5-fold higher in CD8⁻ $\gamma\delta$ T cells as opposed to only five genes in CD8⁺ $\gamma\delta$ T cells (Table V). Furthermore, the expression profile of CD8⁻ $\gamma\delta$ T cells included genes involved in cell cycle regulation such as cyclin-dependent kinase-5, cell cycle check point proteins such as ornithine decarboxylase, and protein translation-associated ribosomal proteins and translation elongation factors. Additional evidence of the activated phenotype of CD8⁻ $\gamma\delta$ T cells was the higher expression of the transcription factor NF- κ B and its anti-apoptotic target genes Bcl-x_L and Bcl-2, and the IL-2R (Table V). In contrast to CD8⁻ $\gamma\delta$ T cells, CD8⁺ $\gamma\delta$ T cell showed a 6-fold greater expression (47 vs 8 tags) of the prohibitin-related protein, BAP 37, a molecule initially described as a B cell receptor-associated molecule that is involved in inhibition of cell proliferation (31). BAP 37 expression is consistent with the less activated/proliferative phenotype of CD8⁺ $\gamma\delta$ T cells. Differential expression of ornithine decarboxylase, selenoprotein, nocturnin, IL-2R, and Bcl-x_L was confirmed by RT-PCR or FACS (Fig. 2, Table III, and data not shown).

Table III. Gene expression patterns predicted by SAGE and analyzed on protein level by flow cytometry

Tag Sequence	CD8 ⁻	CD8 ⁺	Identification	Mean Fluorescence ^a			
				Resting		Activated	
				CD8 ⁻	CD8 ⁺	CD8 ⁻	CD8 ⁺
TCTATCCCTG	76	64	MHC I	300	282	476	370
ACCTTGGAAA	12	1	CD44	337	137	724	520
GTAAGGGCCA	5	6	CD18	15	12	72	54
TATGTGACTA	7	0	IL-2R	315	88	330	211
GGCAAAAAA	5	1	TCR δ -chain	330	92	368	87

^a Multicolor flow cytometric analysis was performed using Ab against the indicated Ag. Values reflect the mean fluorescence of the staining on each subset minus the background mean fluorescence of negative controls. Background ranged from 3–6 mean fluorescence units. Results are representative of at least three separate experiments.

Identification of differentially expressed genes encoding cell surface molecules on immune cells and secreted molecules by SAGE

Genes for a number of different cell surface molecules on immune cells, such as MHC Ags, adhesion molecules, cytokine receptors, and TCRs, were identified, and some were differentially expressed between the two cell types (Table VI). Examples of differentially expressed genes included CD44, semaphorin 4D, scavenger receptor 1, TCR δ -chain, and IL-2R, all of which, except CD63, were higher in CD8⁻ $\gamma\delta$ T cells. As expected, based on previous studies (9, 32), $\alpha\beta$ TCR transcripts were represented in both $\gamma\delta$ T cell subset SAGE libraries (Table VI).

Analysis of secreted molecules showed few examples of differentially expressed genes between the two subsets. A total of 16 unique tag sequences, which represented both pro- and anti-inflammatory genes, and genes encoding pituitary and hypothalamic neuropeptides and plasminogen activator inhibitor were identified (Table VI). Genes that were differentially expressed included galectin-1, prolactin, and IgE-dependent histamine-releasing factor, which were >5-fold higher in CD8⁻ cells, and epider-

mal growth factor, IL-10, and Gro- γ , which were >5-fold higher in CD8⁺ cells. Other genes, such as IL-1, were also differentially expressed, but below the 5-fold level threshold (Table VI). Confirmation experiments were performed for IL-1, CD44, TCR, CD18, MHC class I, and galectin 1. Real-time RT-PCR confirmed the slightly higher expression of IL-1 on CD8⁺ $\gamma\delta$ T cells and the significantly higher expression of galectin-1 on CD8⁻ $\gamma\delta$ T cells (Fig. 2). FACS analysis of resting and PMA/ionomycin-stimulated cells showed that CD44 and TCR were more highly expressed on CD8⁻ $\gamma\delta$ T cells, and CD18 and MHC class I were the same on the two subsets, consistent with the SAGE results (Table III).

Overall, these analyses suggest that $\gamma\delta$ T cells express surface Ags and produce soluble factors that influence not only the immune system, but the nervous, endocrine, and coagulation systems as well.

$\gamma\delta$ T cells express genes normally associated with myeloid cells

A striking observation was the finding that myeloid-associated genes were identified in both subsets by the SAGE analysis. For example, myeloid surface Ags, such as scavenger receptor CD68,

Table IV. Thirty most abundant SAGE tags from both libraries

Tag Sequence	CD8 ⁻	CD8 ⁺	Total	Annotation
AAGGTGGAGG	1222	444	1666	Bovine connexin 43
AGGCGAGATC	817	160	977	Proteasome subunit α type 7
GAGATCCGCA	466	82	548	Multiple hits
GGGCTGGACG	436	26	462	Multiple hits
TGAGAACATT	128	239	367	Ubiquinol cytochrome-c reductase
CTGGGAAATT	234	130	364	Bovine mRNA chromosome 3 with unknown function
AGGAAAGCGG	271	82	353	Ribosomal protein L36
TCGGTCTGGG	259	90	349	Ribosomal protein S2
GTATTCCCCT	235	89	324	Unidentified EST
AACAGGTCCC	166	137	303	Bovine mRNA elongation factor 1 α
ACCTCGGCC	186	58	244	EST, weekly similar to inducible poly(A)-binding protein
GACACCAACT	180	56	236	Ubiquitin specific protease, proto-oncogene
CTGAACATCT	154	70	224	Acidic ribosomal phosphoprotein P2 mRNA
CGCTGGTTCC	173	45	218	Ribosomal protein L11
GCCCCCAATA	186	24	210	Galectin 1
ACAATGACCG	101	103	204	Unidentified EST
GGGCGAGGGG	141	40	181	Jun B proto-oncogene
GCCAACGGTG	109	64	173	Highly similar to human spliceosome-associated protein 114
TTTGAAGAAA	124	38	162	Cytochrome-c oxidase subunit IHQ (VIIb) mRNA
GGAATCAGAG	97	59	156	Unidentified EST
TCTATCCCTG	76	64	140	Bovine MHC I-related mRNA sequence
CCCGGTGCTG	119	21	140	mRNA, mit-ATP synthase proteolipid P1 subunit precursor
CTGTACATTT	62	77	139	Unidentified EST
GGGCTGGACG	89	39	128	Unidentified EST
CGGGACGCAC	116	12	128	Moderately similar to immunoreactive autoantigen-1
AAGGTGGAGG	95	24	119	Highly similar to human elongation factor 1 γ
TTTATGAAGA	38	78	116	Splicing factor 3b, subunit 1
GAGATCCGCA	90	20	110	Unknown
CAGCCAGGG	24	83	107	Weakly similar to cyclic nucleotide gated cation channel
AGGCGAGATC	92	15	107	Unidentified EST

Table V. Differentially expressed genes involved in cell activation, transcription and translation regulation, and protein processing in CD8⁻ vs CD8⁺ $\gamma\delta$ T cells^a

	Identification	CD8 ⁻	CD8 ⁺	Ratio ^b
Higher in CD8 ⁻	H33 human histone	51	0	51.00
	EF1D elongation factor 1 δ	21	0	21.00
	HSP 90 β	21	0	21.00
	Elongin c	20	0	20.00
	I κ B	17	1	17.00
	Ribosomal protein L38	83	5	16.60
	Ribosomal protein L10 A	33	2	16.50
	HSP, 90 kDa	13	1	13.00
	NF κ B	12	0	12.00
	Ribosomal protein L30	22	2	11.00
	Bcl-2 related	10	0	10.00
	Nocturnin (CCR4 homolog)	9	1	9.00
	Ribosomal protein S14	9	1	9.00
	Bcl-x _L	8	0	8.00
	Cyclin-dependent kinase activator 5	8	0	8.00
	Small ribonuclear protein E	8	1	8.00
	Ubiquitin-conjugating enzyme E2G	8	0	8.00
	Galectin 1	186	24	7.75
	Prefoldin subunit 2	31	4	7.75
	IL-2R	7	0	7.00
	Ribosomal protein L7	7	0	7.00
	Ribosomal protein S15	7	0	7.00
	HSP, 79 kDa	32	5	6.40
	Heterogenous ribonuclear protein U	36	6	6.00
	PSD3	6	0	6.00
	Ribosomal protein L8	24	4	6.00
	Small nuclear ribosomal protein B'	6	1	6.00
	Ornithine decarboxylase	17	3	5.67
	cpn 10	16	3	5.33
	BLIMP1	5	1	5.00
	MYB-binding protein 1 a (p160)	5	0	5.00
	POP2	5	1	5.00
	Proteasome subunit α type 7	25	5	5.00
Ribosomal protein S3a	5	0	5.00	
Higher in CD8 ⁺	Histone MACROH2A1	1	5	0.20
	BAP 37/C10	8	47	0.17
	Cysteine-rich intestinal protein	2	12	0.17
	HSP, 70 kDa	1	7	0.14
	TBX2 protein	1	7	0.14
	U2 snRNP auxiliary factor small chain	0	10	0.10

^a HSP, heat shock protein; TBX2, thromboxane 2; MYB, oncogene of avian myeloblastosis virus.

^b Ratio is the number of CD8⁻ tags divided by number of CD8⁺ tags.

CD14 (confirmed by real-time RT-PCR; Fig. 2), and scavenger receptor 1, as well as cytokines known to support myeloid cell differentiation and activation, such as GM-CSF and G-CSF, were detected (Table VI). Another molecule identified was the IgE-dependent, histamine-releasing factor, a novel cytokine associated with activation and subsequent histamine release in basophils and mast cells in the context of allergic reactions. Of particular interest was the finding that the transcriptional repressor BLIMP-1, which is considered an important regulator of myeloid cell and B cell differentiation, was expressed in both subsets, although CD8⁻ $\gamma\delta$ T cells had higher tag numbers (Table V and Fig. 2). Since BLIMP-1 expression is thought to be restricted to myeloid cells and B cells, confirmation of this observation was tested by two approaches. First, BLIMP-1 transcripts were detected by real-time RT-PCR in both subsets; however CD8⁻ $\gamma\delta$ T cells expressed higher levels (Fig. 2). As another means of confirming these observations, an RNase protection assay using a 236-bp BLIMP-1 antisense RNA probe was performed. BLIMP-1 expression was compared in $\gamma\delta$ T cells and $\gamma\delta$ -depleted, $\alpha\beta$ -enriched lymphocytes. As shown in Fig. 3, a significantly stronger BLIMP-1 signal was detected in 4-h PMA/ionomycin-stimulated $\gamma\delta$ T cell RNA, as opposed to in the $\alpha\beta$ T cell-enriched RNA sample (CD2-positive, non- $\gamma\delta$ T cells). Furthermore, the BLIMP-1 signal of $\sim 1 \mu\text{g}$ of $\gamma\delta$ RNA compared with a signal between 1 and 3 μg of PBMC standard

RNA. Thus, $\gamma\delta$ T cells contributed the largest amount of BLIMP-1 transcript in the RNA from total PBMCs.

Discussion

SAGE was used to analyze the functional potential of two bovine $\gamma\delta$ T cell subsets isolated from peripheral blood. Until now, the only genomic studies of $\gamma\delta$ T cells have focused on tissue cells isolated from the intraepithelial lining of the murine gut mucosa (17, 19). By focusing on cells within the blood and subsets known to localize to distinct tissues, functional differences that relate primarily to the T cells themselves were identified, vs those differences that are generated and maintained once the cell enters into a tissue and responds to that tissue environment. Based on this initial analysis, new insights into the functional potential of $\gamma\delta$ T cells as a whole cell class as well as insights into considerable differences in gene expression in circulating $\gamma\delta$ T cell subsets have been gained. Although the antigenic characteristics of the two subsets are not absolute, for the most part the sorted GD3.5⁺ and GD3.5⁻ cells are defined by expression or lack of expression of CD8 (16). As such, we focus our discussion on CD8⁺ and CD8⁻ cells, with the caveat that conclusions concerning the CD8⁺ cells probably hold for the GD3.5⁻, CD8⁻, CD2⁺ subset described by others (33), which was a minor population in the animals used in this study.

Table VI. Immune cell surface Ag (A) and secreted molecules (B) identified by SAGE in $CD8^+$ and $CD8^-$ $\gamma\delta$ T cells

Identification	CD8 ⁻	CD8 ⁺	Total	Description
A.				
MHC I-related	76	64	140	Ag presentation
ICAM 1 (bovine)	23	16	39	Adhesion molecule
MHC III	20	13	33	HLA-B-associated protein 2
MHC I hiro 22.3	19	6	25	Ag presentation
CD44	12	1	13	Adhesion molecule
Scavenger receptor I	10	0	10	Binding and phagocytosis of bacteria (macrophage)
TCR β -chain	8	9	17	TCR
CD68	7	1	8	Macrosialin, macrophage-specific marker
IL-2R	7	0	7	IL-2R α -chain
CD18	6	5	11	Adhesion molecule
CD14	5	4	9	Myeloid membrane protein (macrophage-specific)
Lu-ECAM	5	13	18	Lung endothelial adhesion molecule
TCR δ -chain	5	1	6	$\gamma\delta$ TCR
β_2 -Microglobulin	4	8	12	MHC1-associated molecule
MHC I D18.3	4	1	5	Ag presentation
Semaphorin 4D	4	1	5	CD100, enhances immune responses by binding to CD72
CD63	3	10	13	Lysosomal membrane protein involved in cell signaling
Ig μ -chain C	2	5	7	Ig-related
B.				
Galectin 1	186	24	210	Apoptosis inducing by cross-linking of CD7 and CD45
TNF	109	64	173	TNF
G-CSF	18	4	22	G-CSF
Prolactin-like	11	0	11	Pituitary hormone, known to be involved in autoimmunity
IgE-dependent HRF	9	1	10	B cell growth factor, basophil activation
PAI	4	8	12	Plasminogen activator inhibitor
MDPK ECIP 1	4	5	9	Epithelial cell inflammatory protein
IL-1 β	3	10	13	Proinflammatory cytokine
GM-CSF	3	0	3	GM-CSF
Endothelin-converting enzyme	2	0	2	Endothelin-converting enzyme (vasoconstrictor, neuropeptide)
Epidermal growth factor	1	5	6	Epidermal growth factor
MCH precursor	1	4	5	Melanin-concentrating hormone, involved in leptin regulation
IFN-1 β	1	1	2	Antiviral cytokine
GCP-2	1	2	3	Granulocyte chemotactic protein 2
IL-10	0	6	6	Anti-inflammatory cytokine
Groy	0	4	4	Oncogene and granulocyte chemoattractant

Although a standard method of maximizing gene expression using PMA/ionomycin was used, the comparisons in this study were focused on differences between the two cell populations, not the role of cellular activation. A separate study is being conducted that addresses the role of mitogen (Con-A/IL-2) activation on gene expression in $\gamma\delta$ T cells. Despite the low overall percentage of identified tags (due to working in the bovine system), we gained information on 2000 or more identified genes and/or ESTs for each

library. Over 460 unique tags were represented at least 5-fold higher in one or the other subset. A considerable number of expected genes, based on earlier studies, were identified, but the level of coverage in this first study was not sufficient to identify some genes known to be differentially regulated at the protein level in $CD8^+$ and $CD8^-$ $\gamma\delta$ T cells, such as CD8, CD2, WC1, and CD6. This suggests that as we generate more SAGE tags, and as bovine databases are expanded, many additional, regulated genes will be identified.

One striking observation that came from the SAGE analysis was the difference in the overall functional and/or activation status of the circulating $CD8^-$ vs $CD8^+$ $\gamma\delta$ T cells. $CD8^-$ $\gamma\delta$ T cells showed significantly higher tag numbers for genes involved in transcriptional and translational regulation, proliferation, and inhibition of apoptosis. These differences were evident with or without the PMA stimulation. For example, IL-2R was much higher on both unactivated and PMA-stimulated $CD8^-$ vs $CD8^+$ $\gamma\delta$ T cells. Furthermore, these findings are in agreement with and complement a recently performed cDNA array analysis of Con A/IL-2-activated $CD8^+$ vs $CD8^-$ $\gamma\delta$ T cells, which showed the same activation differences of the two subsets (52). In their recent study Shires et al. (19) described $\gamma\delta$ IEL compared with $\alpha\beta$ IELs in the mouse to be in a resting yet activated state, meaning that $\gamma\delta$ T cells express in high abundance molecules involved in cytotoxicity such as Fas ligand and granzymes, but low amounts of cytokines. It may be that circulating $CD8^-$ $\gamma\delta$ T cells are in a preactivated or activated/resting state as well, which allows these cells to more rapidly respond to external stimuli. Indeed, our previous studies have

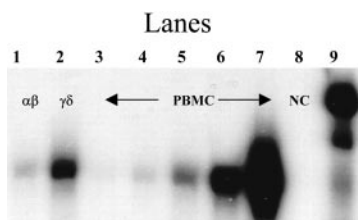


FIGURE 3. Selective BLIMP-1 expression in $\gamma\delta$ T cells. Results of an RNase protection assay confirming BLIMP-1 expression in PMA/ionomycin-activated, purified $\gamma\delta$ T cells is shown. $\gamma\delta$ T cell RNA is compared with RNA from an activated $\alpha\beta$ T cell-enriched preparation, a standard curve of RNA from total PBMCs, and a yeast RNA negative control. Protected RNA samples were loaded on the gel as follows: lane 1, 1.0 μg of RNA from $\alpha\beta$ -enriched lymphocytes; lane 2, 1.0 μg of RNA from total $\gamma\delta$ T cells; lane 3, 0.1 μg of RNA from PBMC; lane 4, 0.3 μg of RNA from PBMC; lane 5, 1.0 μg of RNA from PBMC; lane 6, 3.0 μg of RNA from PBMC; lane 7, 10.0 μg of RNA from PBMC; lane 8, 30 μg of irrelevant yeast RNA; and lane 9, undigested probe. Results are representative of at least three experimental repeats.

found that bovine CD8⁻ $\gamma\delta$ T cells respond rapidly to acute inflammatory and mitogenic stimuli (16). They also show a high level of random migration in *in vitro* migration assays (E. A. Wilson and M. A. Jutila, unpublished observations). Even though they express less CxCR4 receptor than CD8⁺ $\gamma\delta$ T cells, CD8⁻ cells respond equally well, if not better, to the CxCR4 ligand SDF-1 α (34) (E. Wilson and M. A. Jutila, unpublished observations).

Based on the SAGE analysis, one gene that could contribute to the differences in the activation status of CD8⁻ vs CD8⁺ $\gamma\delta$ T cells is BAP 37, a prohibitin-related molecule involved in inhibition of cell proliferation and RNA translation efficiency (31, 35). SAGE analyses showed BAP 37 to be significantly higher in CD8⁺ $\gamma\delta$ T cells as opposed to the CD8⁻ $\gamma\delta$ T cell subset. BAP 37 was originally defined in B cells, and its expression in $\gamma\delta$ T cells suggests a wider role for this molecule in regulating immune cell activity.

Another novel finding in our SAGE analysis was the differential expression of galectin-1, originally described to be expressed on epithelial and vascular endothelial cells (36, 37). Based on SAGE, real-time RT-PCR, and semiquantitative RT-PCR (data not shown), galectin-1 is expressed in $\gamma\delta$ T cells and 2- to 5-fold higher in the CD8⁻ $\gamma\delta$ T cell population. Galectin-1 is a soluble, secreted lectin that has been shown to be involved in the induction of apoptosis of thymocytes and activated T cells. Its expression in thymic epithelial cells and endothelial cells induces death of adherent T cells in a carbohydrate-dependent manner (36, 37). Galectin-1 expression by CD8⁻ $\gamma\delta$ T cells suggests a novel role in the regulation, particularly down-regulation, of the adaptive immune response by these cells.

Of considerable interest, several genes normally associated with myeloid cells were expressed in, and some were differentially expressed between, the two $\gamma\delta$ T cell subsets. CD14, CD68, and macrophage scavenger receptor 1 were represented by significant numbers of SAGE tags in the two libraries. CD14 transcripts are expressed by bovine $\gamma\delta$ T cells, as shown here by RT-PCR and SAGE, and CD8⁻ $\gamma\delta$ T cells bind FITC-labeled *Escherichia coli* through a polyinosinic acid inhibitable receptor, a characteristic of scavenger receptors (N. Meissner, unpublished observations). This finding is not restricted to bovine cells. $\gamma\delta$ T cells from two patients with Crohn's disease express CD14 (38), and we have found that some *in vitro* expanded human $\gamma\delta$ T cells can be induced to express CD14 as well (J. Hedges and M. Jutila, unpublished observations). SAGE also predicted the expression of cytokines produced by and others that act on myeloid cells. An example included IgE-dependent histamine-releasing factor, a B cell growth factor and basophil activator. This basophil activator is expressed in myeloid cells and is involved in delayed-type allergic responses (39). Connexin 43, the most abundant of all SAGE tags in this study, may also indicate a connection with macrophages, since activated macrophages express this gap junction protein (40). Connexin 43 may allow $\gamma\delta$ T cells to form gap junctions with epithelial and/or endothelial cells.

An additional association with the myeloid lineage revealed by our study was the finding that $\gamma\delta$ T cells express the myeloid cell transcription and differentiation factor BLIMP-1. Due to this link, we concentrated on this observation and confirmed BLIMP-1 expression in bovine $\gamma\delta$ T cells by real-time RT-PCR and a quantitative RNase protection assay. Again, this finding does not appear to be restricted to bovine cells. Fahrer and colleagues (17) using cDNA arrays demonstrated BLIMP-1 expression in the intraepithelial $\gamma\delta$ T cells of mice, but not in $\alpha\beta$ T cells isolated from the same location. These findings are surprising, since the expression of BLIMP-1 was initially described as an important transcriptional repressor in B cells, driving B cell differentiation into a plasma

cell. In addition, BLIMP-1 expression has been shown to be a trigger for differentiation of the myeloid lineage. Two important targets of this repressor have been so far described: c-Myc and CIITA, a coactivator for MHC II complex (41–43). BLIMP-1 expression in cells is repressed by BCL-6, which also represses CD44 expression (44). The observation that CD44 is highest in CD8⁻ $\gamma\delta$ T cells, in correlation with higher BLIMP-1 expression in this subset, suggests that the regulation of BLIMP-1 in $\gamma\delta$ T cells might be similar to that described in B cells and myeloid cells. Therefore, BLIMP-1 might be functionally important during terminal differentiation of at least some subsets of $\gamma\delta$ T cells, and current studies are focused on defining the control elements involved in its expression.

These new observations support the idea that $\gamma\delta$ T cells are an important bridge between the innate and acquired immune systems (45). Not only do these cells localize in tissues similar to myeloid cells and produce factors that direct the activity of myeloid cells, but they also have apparently retained many of the functional attributes of neutrophils and monocytes. They are recruited to sites of inflammation via adhesion molecules similar to those used by myeloid cells. Unlike naive $\alpha\beta$ T cells, all bovine CD8⁻ $\gamma\delta$ T cells in newborns express E-selectin ligands and migrate to acute and chronic sites of inflammation, like myeloid cells (46, 47). Bovine $\gamma\delta$ T cells are potentially phagocytic via scavenger receptor 1 and might function as professional APC (48–50). Recently, Richards and Nelson (51) postulated, based on a phylogenetic analysis, that the $\gamma\delta$ TCR sequences are the most ancient of the Ag recognition molecules of lymphocytes, and that Ag recognition properties of $\alpha\beta$ cells (TCR) and B cells (Ig) arose from an ancient $\gamma\delta$ T cell. Our findings support this hypothesis and provide additional direct examples of potential functional links between innate (myeloid-derived) and adaptive (lymphoid-derived) immunity provided by $\gamma\delta$ T cells, which warrant further investigation.

Finally, the results of this study as well as results from the only other genomic analyses performed on $\gamma\delta$ T cells to date (17, 18) must be considered in the context of the animal systems in which they were performed (ruminants and rodents). The evolutionary conservation of the $\gamma\delta$ T cell population suggests that common findings between these animal groups will probably extend to humans, but it will be important to perform similar types of studies with human cells. Our results show that analysis of circulating cells, vs isolation of tissue cells, can provide unique insights into the functional differences of $\gamma\delta$ T cell subsets.

Acknowledgments

We thank Larissa Jackiw for her excellent technical expertise in sorting $\gamma\delta$ T cell subsets, Diane Cockrell for preparing $\gamma\delta$ T cell RNA, and Jim Thompson and Kerri Rask for collection of all blood samples. We also thank Dr. James Fox for providing sequencing space and organizing the sequencing of the CD8⁺ $\gamma\delta$ SAGE library at U.S. Department of Agriculture Meat Animal Research Center (Clay Center, NE), as well as Dr. Ed Schmidt for technical advice and support.

References

1. Bank, L., R. A. DePinho, M. B. Brenner, J. Cassimeris, F. W. Alt, and L. Chess. 1986. A functional T3 molecule associated with a novel heterodimer on the surface of immature human thymocytes. *Nature* 322:179.
2. Brenner, M. B., J. McLean, D. P. Dialynas, J. L. Strominger, J. A. Smith, F. L. Owen, J. G. Seidman, S. Ip, F. Rosen, and M. S. Krangel. 1986. Identification of a putative second T-cell receptor. *Nature* 322:145.
3. Saito, H., Y. Kanamori, T. Takemori, H. Nariuchi, E. Kubota, H. Takahashi-Iwanaga, T. Iwanaga, and H. Ishikawa. 1998. Generation of intestinal T cells from progenitors residing in gut cryptopatches. *Science* 280:275.
4. Asarnow, D. M., W. A. Kuziel, M. Bonyhadi, R. E. Tigelaar, P. W. Tucker, and J. P. Allison. 1988. Limited diversity of $\gamma\delta$ antigen receptor genes of Thy-1⁺ dendritic epidermal cells. *Cell* 55:837.

5. Mallick-Wood, C. A., J. M. Lewis, L. I. Richie, M. J. Owen, R. E. Tigelaar, and A. C. Hayday. 1998. Conservation of T cell receptor conformation in epidermal $\gamma\delta$ cells with disrupted primary V γ gene usage. *Science* 279:1729.
6. Zuany-Amorim, C., C. Ruffie, S. Haile, B. B. Vargaftig, P. Pereira, and M. Pretolani. 1998. Requirement for $\gamma\delta$ T cells in allergic airway inflammation. *Science* 280:1265.
7. Payer, E., A. Elbe, and G. Stingl. 1991. Circulating CD3⁺/T cell receptor V γ 3⁺ fetal murine thymocytes home to the skin and give rise to proliferating dendritic epidermal T cells. *J. Immunol.* 146:2536.
8. Wilson, E., B. Walcheck, W. C. Davis, and M. A. Jutila. 1998. Preferential tissue localization of bovine $\gamma\delta$ T cell subsets defined by anti-T cell receptor for antigen antibodies. *Immunol. Lett.* 64:39.
9. Itohara, S., A. G. Farr, J. J. Lafaille, M. Bonneville, Y. Takagaki, W. Haas, and S. Tonegawa. 1990. Homing of a $\gamma\delta$ thymocyte subset with homogeneous T-cell receptors to mucosal epithelia. *Nature* 343:754.
10. Nakajima, S., W. T. Roswit, D. C. Look, and M. J. Holtzman. 1995. A hierarchy for integrin expression and adhesiveness among T cell subsets that is linked to TCR gene usage and emphasizes V δ 1⁺ $\gamma\delta$ T cell adherence and tissue retention. *J. Immunol.* 155:1117.
11. Ferrick, D. A., M. D. Schrenzel, T. Mulvanian, B. Hsieh, W. G. Ferlin, and H. Lepper. 1995. Differential production of interferon- γ and interleukin-4 in response to Th1- and Th2-stimulating pathogens by $\gamma\delta$ T cells in vivo. *Nature* 373:255.
12. Egan, P. J., and S. R. Carding. 2000. Downmodulation of the inflammatory response to bacterial infection by $\gamma\delta$ T cells cytotoxic for activated macrophages. *J. Exp. Med.* 191:2145.
13. O'Brien, R. L., X. Yin, S. A. Huber, K. Ikuta, and W. K. Born. 2000. Depletion of a $\gamma\delta$ T cell subset can increase host resistance to a bacterial infection. *J. Immunol.* 165:6472.
14. Huber, S. A., D. Graveline, M. K. Newell, W. K. Born, and R. L. O'Brien. 2000. V γ 1⁺ T cells suppress and V γ 4⁺ T cells promote susceptibility to coxsackievirus B3-induced myocarditis in mice. *J. Immunol.* 165:4174.
15. Hein, W. R., and C. R. Mackay. 1991. Prominence of $\gamma\delta$ T cells in the ruminant immune system. *Immunol. Today* 12:30.
16. Wilson, E., M. K. Aydintug, and M. A. Jutila. 1999. A circulating bovine $\gamma\delta$ T cell subset, which is found in large numbers in the spleen, accumulates inefficiently in an artificial site of inflammation: correlation with lack of expression of E-selectin ligands and L-selectin. *J. Immunol.* 162:4914.
17. Fahrer, A. M., Y. Konigshofer, E. M. Kerr, G. Ghandour, D. H. Mack, M. M. Davis, and Y. H. Chien. 2001. Attributes of $\gamma\delta$ intraepithelial lymphocytes as suggested by their transcriptional profile. *Proc. Natl. Acad. Sci. USA* 98:10261.
18. Velculescu, V. E., L. Zhang, B. Vogelstein, and K. W. Kinzler. 1995. Serial analysis of gene expression. *Science* 270:484.
19. Shires, J., E. Theodoridis, and A. C. Hayday. 2001. Biological insights into TCR $\gamma\delta$ ⁺ and TCR $\alpha\beta$ ⁺ intraepithelial lymphocytes provided by serial analysis of gene expression (SAGE). *Immunity* 15:419.
20. Jones, W. M., B. Walcheck, and M. A. Jutila. 1996. Generation of a new $\gamma\delta$ T cell-specific monoclonal antibody (GD3.5): biochemical comparisons of GD3.5 antigen with the previously described Workshop Cluster 1 (WC1) family. *J. Immunol.* 156:3772.
21. Howard, C. J., W. I. Morrison, A. Bensaid, W. Davis, L. Eskra, J. Gerdes, M. Hadam, D. Hurley, W. Leibold, and J. J. Letesson. 1991. Summary of workshop findings for leukocyte antigens of cattle. *Vet. Immunol. Immunopathol.* 27:21.
22. Dukas, K., P. Sarfati, N. Vaysse, and L. Pradayrol. 1993. Quantitation of changes in the expression of multiple genes by simultaneous polymerase chain reaction. *Anal. Biochem.* 215:66.
23. Abrahamsen, M. S., and A. A. Schroeder. 1999. Characterization of intracellular *Cryptosporidium parvum* gene expression. *Mol. Biochem. Parasitol.* 104:141.
24. Walcheck, B., M. White, S. Kurk, T. K. Kishimoto, and M. A. Jutila. 1992. Characterization of the bovine peripheral lymph node homing receptor: a lectin cell adhesion molecule (LECAM). *Eur. J. Immunol.* 22:469.
25. Ng, K. H., J. D. Watson, R. Prestidge, and B. M. Buddle. 1995. Cytokine mRNA expressed in tuberculin skin test biopsies from BCG-vaccinated and *Mycobacterium bovis* inoculated cattle. *Immunol. Cell Biol.* 73:362.
26. Peters, D. G., A. B. Kassam, H. Yonas, E. H. O'Hare, R. E. Ferrell, and A. M. Brufsky. 1999. Comprehensive transcript analysis in small quantities of mRNA by SAGE-lite. *Nucleic Acids Res.* 27:e39.
27. Powell, J. 1998. Enhanced concatemer cloning: a modification to the SAGE (serial analysis of gene expression) technique. *Nucleic Acids Res.* 26:3445.
28. Powell, J. 2000. SAGE. The serial analysis of gene expression. *Methods Mol. Biol.* 99:297.
29. Wilson, E., J. F. Hedges, E. C. Butcher, M. Briskin, and M. A. Jutila. 2002. Bovine $\gamma\delta$ T cell subsets express distinct patterns of chemokine responsiveness and adhesion molecules: a mechanism for tissue-specific $\gamma\delta$ T cell subset accumulation. *J. Immunol.* 169:4970.
30. Davis W. C., S. Marusic, H. A. Lewin, G. A. Splitter, L. E. Perryman, T. C. McGuire, and J. R. Gorham. 1987. The development and analysis of species specific and cross reactive monoclonal antibodies to leukocyte differentiation antigens and antigens of the major histocompatibility complex for use in the study of the immune system in cattle and other species. *Vet. Immunol. Immunopathol.* 15:337.
31. Terashima, M., K. M. Kim, T. Adachi, P. J. Nielsen, M. Reth, G. Kohler, and M. C. Lamers. 1994. The IgM antigen receptor of B lymphocytes is associated with prohibitin and a prohibitin-related protein. *EMBO J.* 13:3782.
32. Bischof, A., J. H. Park, and T. Huenig. 2000. Expression of T-cell receptor β -chain mRNA and protein in $\gamma\delta$ T-cells from euthymic and athymic rats: implications for T-cell lineage divergence. *Dev. Immunol.* 8:19.
33. MacHugh, N. D., J. K. Mburu, M. J. Carol, C. R. Wyatt, J. A. Orden, and W. C. Davis. 1997. Identification of two distinct subsets of bovine $\gamma\delta$ T cells with unique surface phenotype and tissue distribution. *Immunology* 92:340.
34. Kantele, J. M., S. Kurk, and M. A. Jutila. 2000. Effects of continuous exposure to stromal cell-derived factor-1 α on T cell rolling and tight adhesion to monolayers of activated endothelial cells. *J. Immunol.* 164:5035.
35. Miyamoto, S., J. Qin, and B. Safer. Detection of early gene expression changes during activation of human primary lymphocytes by in vitro synthesis of proteins from polysome-associated mRNAs. *Protein Sci.* 10:423.
36. Perillo, N. L., K. E. Pace, J. J. Seilhamer, and L. G. Baum. 1995. Apoptosis of T cells mediated by galectin-1. *Nature* 378:736.
37. Pace, K. E., H. P. Hahn, M. Pang, J. T. Nguyen, and L. G. Baum. 2000. CD7 delivers a pro-apoptotic signal during galectin-1-induced T cell death. *J. Immunol.* 165:2331.
38. Dialynas, D. P. and V. D. Rodgers. 2002. Anomalous leukopoiesis in two patients with Crohn's disease. *J. Clin. Gastroenterol.* 34:64.
39. Kang, H. S., M. J. Lee, H. Song, S. H. Han, Y. M. Kim, J. Y. Im, and I. Choi. 2001. Molecular identification of IgE-dependent histamine-releasing factor as a B cell growth factor. *J. Immunol.* 166:6545.
40. Jara, P. I., M. P. Boric, and J. C. Saez. 1995. Leukocytes express connexin43 after activation lipopolysaccharide and appear to form gap junctions with endothelial cells after ischemia-reperfusion. *Proc. Natl. Acad. Sci. USA* 92:7011.
41. Turner, C. A. J., D. H. Mack, and M. M. Davis. 1994. Blimp-1, a novel zinc finger-containing protein that can drive the maturation of B lymphocytes into immunoglobulin-secreting cells. *Cell* 77:297.
42. Chang, D. H., C. Angelin-Duclos, and K. Calame. 2000. BLIMP-1: trigger for differentiation of myeloid lineage. *Nat. Immunol.* 1:169.
43. Calame, K. L. 2001. Plasma cells: finding new light at the end of B cell development. *Nat. Immunol.* 2:1103.
44. Shaffer, A. L., X. Yu, Y. He, J. Boldrick, E. P. Chan, and L. M. Staudt. 2000. BCL-6 represses genes that function in lymphocyte differentiation, inflammation, and cell cycle control. *Immunity* 13:199.
45. Mak, T. W., and D. A. Ferrick. 1998. The $\gamma\delta$ T-cell bridge: linking innate and acquired immunity. *Nat. Med.* 4:764.
46. Jutila, M. A., R. F. Bargatze, S. Kurk, R. A. Warnock, N. Ehsani, S. R. Watson, and B. Walcheck. 1994. Cell surface P- and E-selectin support shear-dependent rolling of bovine $\gamma\delta$ T cells. *J. Immunol.* 153:3917.
47. Jutila, M. A., and S. Kurk. 1996. Analysis of bovine $\gamma\delta$ T cell interactions with E-, P-, and L-selectin: characterization of lymphocyte on lymphocyte rolling and the effects of O-glycoprotease. *J. Immunol.* 156:289.
48. Collins, R. A., D. Werling, S. E. Duggan, A. P. Bland, K. R. Parsons, and C. J. Howard. 1998. $\gamma\delta$ T cells present antigen to CD4⁺ $\alpha\beta$ T cells. *J. Leukocyte Biol.* 63:707.
49. Evans, C. W., B. T. Lund, I. McConnell, and R. Bujdosos. 1994. Antigen recognition and activation of ovine $\gamma\delta$ T cells. *Immunology* 82:229.
50. Hopkins, J., I. McConnell, R. G. Dalziel, and B. M. Dutia. 1993. Patterns of major histocompatibility complex class II expression by T cell subsets in different immunological compartments. II. Altered expression and cell function following activation in vivo. *Eur. J. Immunol.* 23:2889.
51. Richards, M. H., and J. L. Nelson. 2000. The evolution of vertebrate antigen receptors: a phylogenetic approach. *Mol. Biol. Evol.* 17:146.
52. Hedges, J. F., D. Cockrell, L. Jackiw, N. Meissner, and M. A. Jutila. Differential mRNA expression in circulating $\gamma\delta$ T lymphocyte subsets defines unique tissue-specific functions. *J. Leukocyte Biol. In press.*